

SENSITIVITY OF A HEAVY RAIN PRODUCING WESTERN MEDITERRANEAN CYCLONE TO THE INTENSITY AND POSITION OF TWO UPPER-LEVEL POTENTIAL VORTICITY CENTRES

R. Romero

Grup de Meteorologia, Departament de Física, Universitat de les Illes Balears, Palma de Mallorca, Spain. Email: dfsrrm8@ps.uib.es

SUMMARY

A surface cyclone that produced heavy precipitation in the western Mediterranean region on 28-29 September 1994 is numerically simulated. The dynamical forcing at upper levels is strong and appears to be associated with two positive potential vorticity (PV) anomalies that are embedded within the large-scale trough and rotate about each other. The sensitivity of the mesoscale forecast to the initial intensity and position of the anomalies is examined by applying a piecewise PV inversion method and using the inverted balanced fields to generate an ensemble of simulations with perturbed initial conditions. The results show that the track, shape and intensity of the surface cyclone, as well as the rainfall field, are highly sensitive to the characteristics of the anomalies. Finally, the relative roles of the orography and sea surface latent heat flux versus the action of the upper-level PV anomalies are examined with additional simulations.

1. Introduction

The genesis of heavy precipitation is a major meteorological threat in the western Mediterranean region. The strong social and economic impact of the resulting flash floods has motivated numerous observational, diagnostic and numerical modelling research efforts during the last two decades. In particular, several works have taken advantage of the potential offered by mesoscale models and have isolated the role played by different physical factors by means of sensitivity or factor separation techniques. Factors typically considered include the so-called boundary factors, such as local and remote orographies, surface characteristics and surface heat fluxes (e.g. Ramis et al. 1998), and factors associated with the model physics, such as latent heat exchanges in the parameterized moist processes (Romero et al. 2000). Comparatively less attention, however, has been paid to the effects of internal features of the flow dynamics (jet streaks, troughs, fronts, etc.) probably because, unlike the external or parameterization factors, modifying or switching off these elements in the model simulations is not straightforward.

A relatively clean approach to deal with internal dynamical features is based on the concept of potential vorticity (PV) and its invertibility principle (Hoskins et al. 1985). Application of piecewise PV inversion is particularly useful, since once identified, any PV element of interest as well as its associated mass and wind fields can be isolated in a consistent way for diagnostic or prognostic purposes. In particular, piecewise inversion schemes have been applied for initial-value problems, where the effects of incorporating, modifying or removing PV perturbations (i.e. a certain amount of balanced

flow) in the model initial conditions on the subsequent forecast are investigated (e.g. Huo et al. 1999).

Here, the PV approach is used to investigate the sensitivity of a western Mediterranean cyclone to the structure of the upper-level flow. The event (28-29 September 1994) was characterized by the genesis of several mesoscale convective systems over the western Mediterranean waters and the eastern part of Spain, producing important amounts of rainfall near the coasts (Fig. 1). Motivation for the study is based on a control numerical simulation and diagnostic products presented in next section, which show that the upper-level PV field upstream of the western Mediterranean was dominated by two PV centres rotating cyclonically about each other. A piecewise PV inversion methodology is used to examine the sensitivity of the simulation to these PV centres by varying their intensity and position in the model initial conditions.



Fig. 1. Rainfall (mm) in Mediterranean Spain from 07 UTC 28 September 1994 to 07 UTC 30 September 1994.

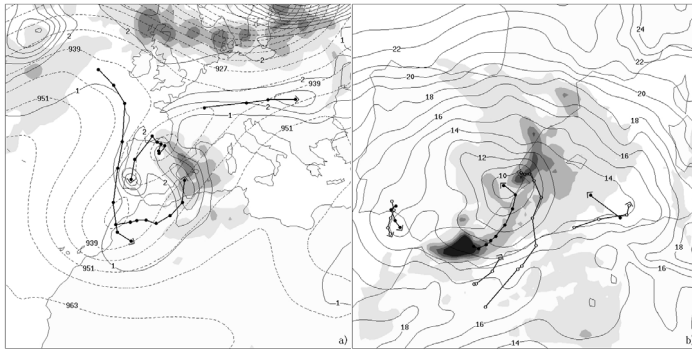


Fig. 2. Control simulation: (a) Geopotential height at 300 hPa at 06 UTC 28 September (dashed, in dam); Ertel's potential vorticity on the 330 K isentropic surface at 00 UTC 30 September (continuous line, in PVU), with an indication of trajectories at 6 h intervals of several maxima present at that time (circles); and maximum value of the low tropospheric (1000-700 hPa) temperature advection during the simulation (shaded, for values exceeding 0.2, 0.4 and 0.6 K h⁻¹). (b) Sea level pressure at 00 UTC 30 September (continuous line, in hPa without the leading 10), with an indication of back trajectories at 3 h intervals of several minima (circles, with open circles for minima dissipated before that time); and total precipitation (shaded, for values exceeding 10, 40, 70, 100 and 130 mm).

2. Control simulation and discussion

The event was numerically simulated using the non-hydrostatic version of the MM5 mesoscale model (Grell et al. 1995). Two interacting domains with horizontal resolutions of 60 and 20 km were used (those shown in Figs. 2a and b, respectively). The simulation presented covers 48 h, starting at 00 UTC 28 September 1994. Initial and boundary conditions are based on the global analysis from the NCEP, available at 00 and 12 UTC on standard isobaric surfaces.

The most relevant results of this simulation are summarized in Fig. 2. Note the complex structure of the initial upper-level wave (Fig. 2a), since, embedded within the large-scale trough, there are two geopotential height minima centered near the Gulf of Vizcaya and the Moroccan Atlantic coast. Calculation of Ertel's potential vorticity (Ertel 1942)

reveals that the two embedded lows are each associated with a PV maximum, as expected. Figure 2a displays the trajectories of these PV centres on the 330 K isentropic surface during the simulation, as well as their structure and position at the end of the period. Observe that, while rotating about each other, the PV centres migrate toward southern Portugal and the western Mediterranean, respectively. This movement implies high values of PV advection at upper levels over the western Mediterranean and eastern part of Spain progressing from south to north (not shown). Associated with the evolution at upper-levels, warm air advection in the lower troposphere during the simulation is maximized over the western Mediterranean and eastern Spain (see shaded field in Fig. 2a), again with the maximum of this field progressing from south to north.

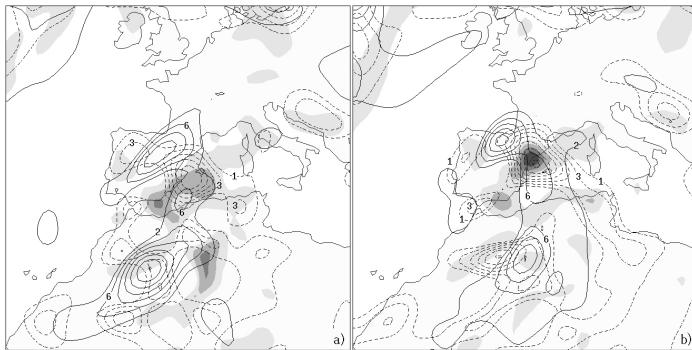


Fig. 3. Control simulation: Mid-upper tropospheric (700-200 hPa) upward quasigeostrophic forcing (continuous line, starting at $2 \cdot 10^{-18} \text{ m kg}^{-1} \text{ s}^{-1}$ every $4 \cdot 10^{-18} \text{ m kg}^{-1} \text{ s}^{-1}$); low tropospheric (1000-700 hPa) upward quasigeostrophic forcing (dashed line, starting at $1 \cdot 10^{-18} \text{ m kg}^{-1} \text{ s}^{-1}$ every $2 \cdot 10^{-18} \text{ m kg}^{-1} \text{ s}^{-1}$); and water vapor flux convergence in the layer 1000-700 hPa (shaded, for values exceeding 0.1, 0.5, 1 and $1.5 \text{ g m}^{-2} \text{ s}^{-1}$): (a) At 00 UTC 29 September. (b) At 12 UTC 29 September.

Calculation of quasigeostrophic forcing for vertical motion (Fig. 3) reveals that the evolution of the upper-level PV field and the low-level temperature advection field are associated with important centres of dynamic forcing for upward motion in the mid-upper and lower troposphere, respectively. These areas of positive forcing overlap over the western Mediterranean and eastern Spain, and the overlapping zone moves northwards during 28-29 September. In addition, the model forecasts intense values of water vapor flux convergence at low levels in the same areas (shaded field in Fig. 3).

Since convective instability was also present, the synoptic environment was highly supportive for the development and maintenance of convection.

In response to the previous dynamical forcing pattern, an intense cyclonic development is forecast over the western Mediterranean and Iberian peninsula (Fig. 2b). The skill of the model for capturing spatial and quantitative details of the rainfall field over Mediterranean Spain is also remarkable (compare shaded field with Fig. 1). It is interesting to note that, unlike many cases of flash flood events in eastern Spain, characterized by

relatively stationary surface lows near the Algerian coast, in this case the disturbance is mobile and progresses northwards from that genesis area to the coast of Valencia.

Although the two embedded upper-level PV centres identified on Fig. 2a seem to be playing an important role for the evolution, intensity and areal extent of the surface cyclone, there is no practical

way, with a single control simulation, of quantifying the degree of dependence of the mesoscale forecast on the specific structure of the upper-level flow. It would be interesting to investigate how a potential error in the representation of these PV centres might affect the mesoscale forecast. With this aim, a sensitivity analysis based on additional simulations with perturbed initial conditions is carried out.

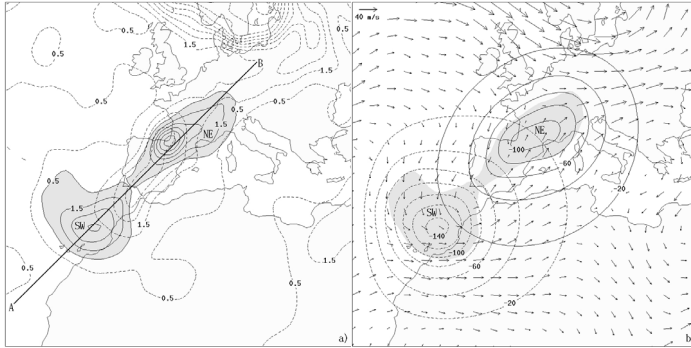


Fig. 4. (a) Ertel's potential vorticity at 250 hPa corresponding to the SW and NE anomalies (continuous line, starting at 0.5 PVU every 1 PVU) and the total field without the anomalies (dashed, starting at 0.5 PVU every 1 PVU). (b) Streamfunction at 250 hPa of the balanced flow derived from inversion the SW and NE PV anomalies (dashed and continuous line respectively, starting at $20 \cdot 10^5 \text{ m}^2 \text{ s}^{-1}$ every $-20 \cdot 10^5 \text{ m}^2 \text{ s}^{-1}$); and vector wind field at 250 hPa corresponding to the total flow without the balanced components associated with the anomalies or background flow (a reference vector is shown in the upper left corner).

3. Sensitivity to the upper level PV anomalies

The method used to explore the sensitivity of the mesoscale simulation to the upper-level PV centres, for convenience referred to as SW and NE PV centres (Fig. 4a), requires the calculation of a balanced flow associated with each anomaly. The piecewise PV inversion technique of Davis and Emanuel (1991) was used for such purpose.

The technique was applied to invert the SW and NE PV anomalies at 00 UTC 28 September 1994 - the simulation start time. The perturbation PV field was defined as the departure from the 6-day time average about 00 UTC 28 September, and the pieces representing the two anomalies were identified as the volumes of positive PV perturbation above 500 hPa present to the southwest and northeast of the Gulf of Cádiz. Figure 4a shows the structure of the SW and NE anomalies at 250 hPa, as well as the background PV field at the same level. The selected reference or mean state is such that, even without the anomalies, the PV field is still characterized by the intrusion of a tongue of high PV towards the Iberian peninsula, since we are interested in manipulating the two embedded upper-level lows that are shaping

the large-scale trough (Fig. 2a), not the trough itself (represented by the high-PV tongue).

An horizontal view for 250 hPa of the inverted circulations and background flow is included in Fig. 4b. Clearly, the effect of the background flow is to advect the SW anomaly towards the western Mediterranean and to stretch the NE anomaly along the SW-NE direction. The circulations associated with the anomalies are contributing to their self-rotation and to the cyclonic rotation -or negative tilting- of the main trough. To a lesser extent, the anomalies are also contributing to advect each other along a cyclonic path. All these lateral interactions are consistent with the evolution of the upper-level flow observed in the control simulation (Fig. 2a).

A vertical cross section of the inverted balanced fields (Fig. 5) illustrates that the localized PV anomalies are felt throughout the entire atmospheric column. This emphasizes that a potential error in resolving the upper-level PV centres would be reflected not only at the anomaly level, but down to the surface level, affecting key fields for surface cyclogenesis and forcing of vertical motion such as the temperature advection pattern.

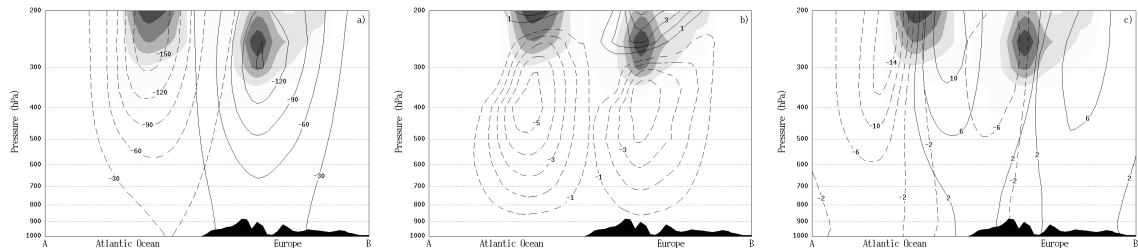


Fig. 5. Vertical cross section along the line AB shown in Fig. 4a of the PV-inverted fields from the SW and NE anomalies: (a) Geopotential height (dashed and continuous contours for the SW and NE anomalies respectively, starting at -30 m every -30 m); (b) Temperature (continuous line for positive values and dashed line for negative values, in $1 \text{ }^\circ\text{C}$ intervals starting at 1 and $-1 \text{ }^\circ\text{C}$, respectively); and (c) Section-normal winds (continuous line for flow into the page and dashed line for flow out of the page, in 4 m s^{-1} intervals starting at 2 and -2 m s^{-1} , respectively). The SW and NE PV anomalies are shown as shaded for values exceeding 0.5, 1.5, 2.5, 3.5 and 4.5 PVU.

The sensitivity experiments were designed by adding and/or subtracting the PV-inverted balanced fields (geopotential, temperature and wind) into the model initial conditions. The relative humidity field was kept unaltered. Two sets of simulations were designed to study separately the sensitivity of the forecast to the intensity and position of the anomalies (Tables 1 and 2, respectively). In the first set, the SW and NE anomalies are either doubled (adding the inverted fields), removed (subtracting the fields) or kept unchanged. In the second set, the intensity of the anomalies is not changed but the position is shifted along the AB axis shown in Fig. 4a. The anomalies are either moved outwards (by subtracting the associated fields and adding them 425 km farther from the Iberian peninsula), moved inwards (in the same way except 425 km closer to the Iberian peninsula) or kept in the original position. The results of these 16 simulations are shown in Figs. 6 and 7, which can be compared with the control run shown in Fig. 2b.

Table 1. Sensitivity to the intensity of the PV anomalies

Experiment	SW anomaly	NE anomaly
<i>S00</i>	Removed	Removed
<i>S22</i>	Doubled	Doubled
<i>S10</i>	Unchanged	Removed
<i>S20</i>	Doubled	Removed
<i>S01</i>	Removed	Unchanged
<i>S02</i>	Removed	Doubled
<i>S21</i>	Doubled	Unchanged
<i>S12</i>	Unchanged	Doubled

Table 2. Sensitivity to the position of the PV anomalies

Experiment	SW anomaly	NE anomaly
<i>S--</i>	Inwards	Inwards
<i>S++</i>	Outwards	Outwards
<i>S=-</i>	Unchanged	Inwards
<i>S+-</i>	Outwards	Inwards
<i>S-=</i>	Inwards	Unchanged
<i>S-+</i>	Inwards	Outwards
<i>S+=</i>	Outwards	Unchanged
<i>S=+</i>	Unchanged	Outwards

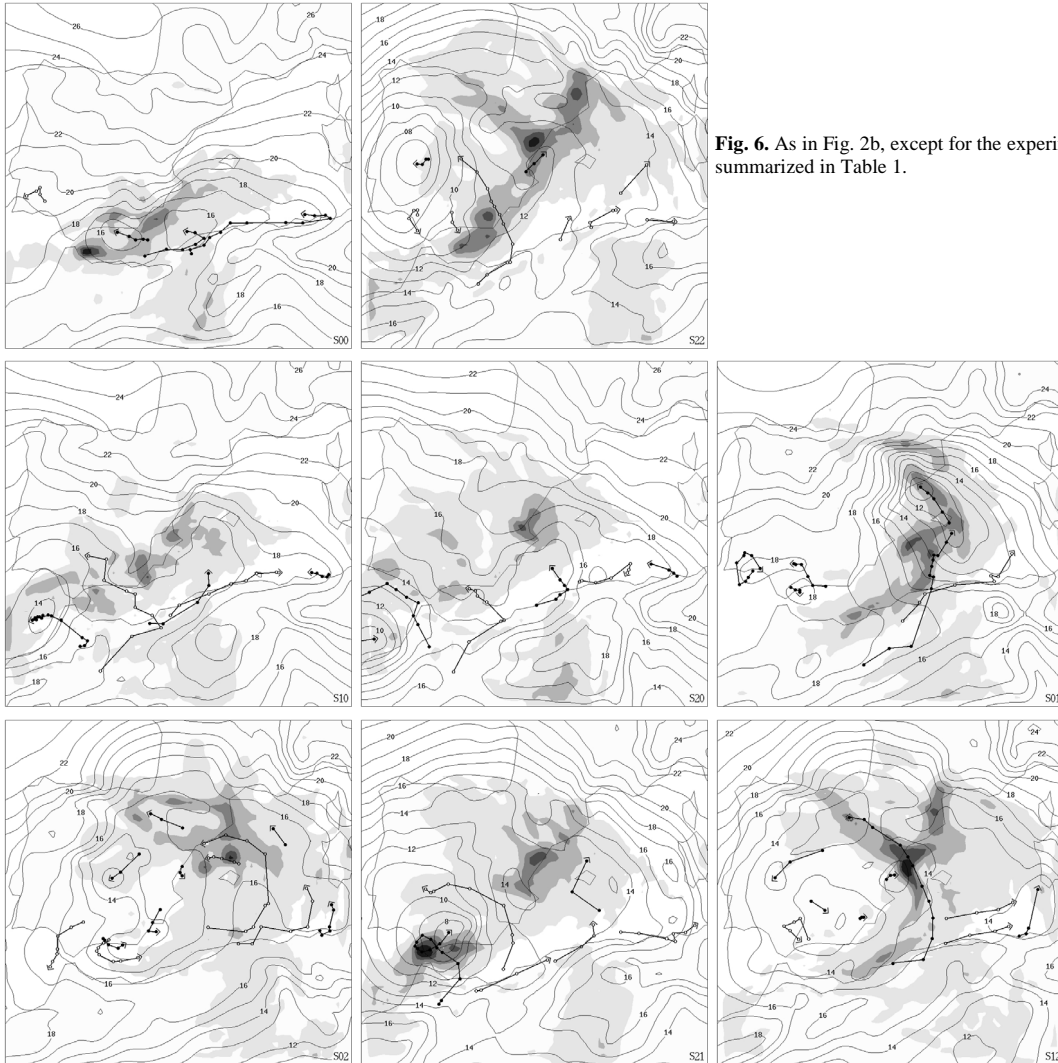


Fig. 6. As in Fig. 2b, except for the experiments summarized in Table 1.

The designed experiments clearly illustrate the importance of the two embedded upper-level PV anomalies for the track, shape and intensity of the surface cyclone and the corresponding rainfall pattern. In particular, the experiments with the anomalies removed or moved away from each other ($S00$, $S10$, $S++$ and $S=+$) result in synoptically weak scenarios, characterized by stationary surface lows extended along the lee of the Atlas mountains and with most of the rainfall restricted to the southern Mediterranean areas. At the other end, the experiments with enhanced PV structures aloft (e.g. $S22$, $S--$, $S=-$ and $S=-$) result in extensive and very mobile surface disturbances that generate heavy rain in the northern Mediterranean zones as well. And experiments in which the relative weight of the

northern anomaly is enhanced ($S01$, $S02$, $S12$, $S+=$) produce cyclones that evolve farther east and north of southeastern Spain, thus inducing a concentration of most of the rainfall in northern Mediterranean areas. Interestingly, more distinct behaviors are found with perturbed *intensities* of the anomalies than with perturbed *positions*, although this can be in part related to the arbitrariness involved with the definition of the perturbations. On the other hand, the sea level pressure field generally exhibits higher sensitivity to the perturbed anomalies than the rainfall field, probably because precipitation generation is largely controlled, under easterly regimes, by the interaction of the moist flow with the virtually "error-free" coastal topographic features.

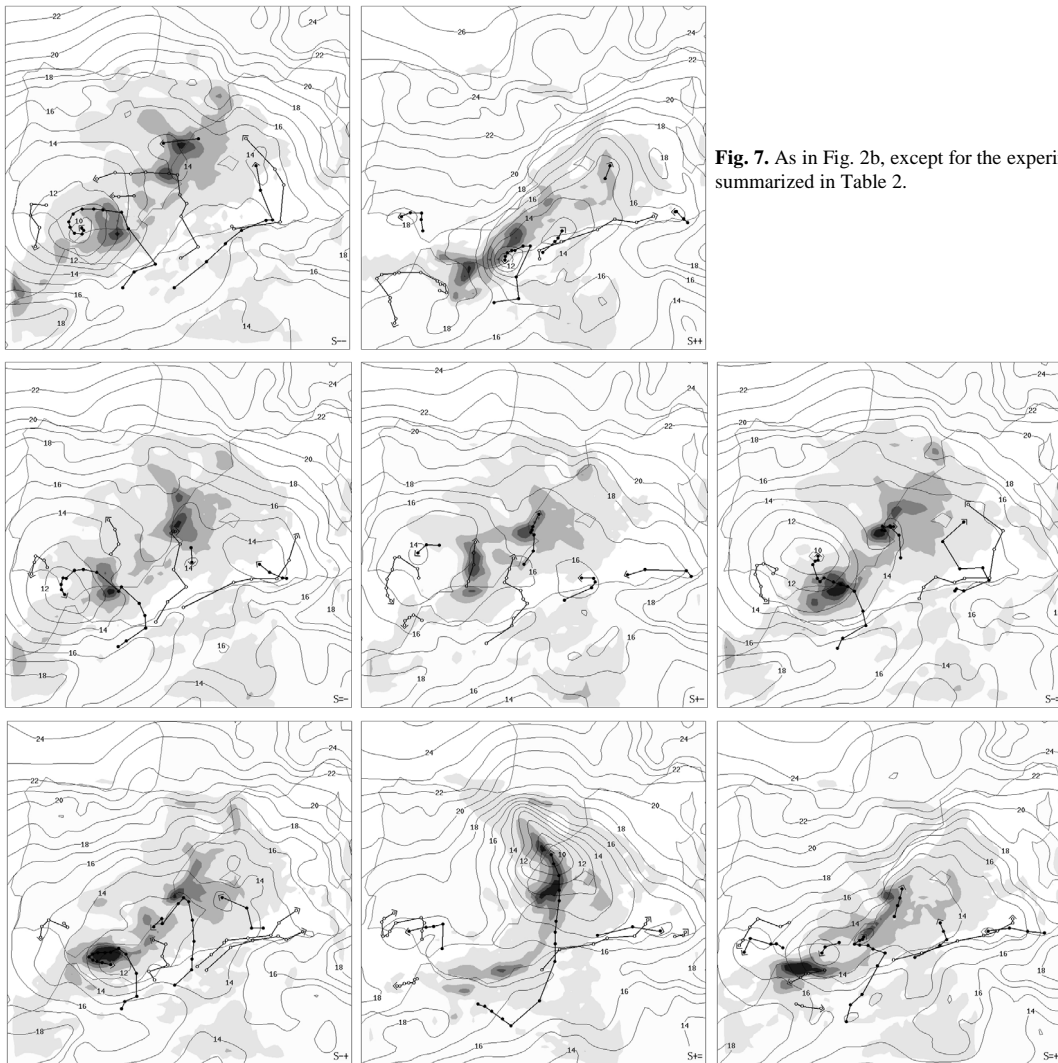


Fig. 7. As in Fig. 2b, except for the experiments summarized in Table 2.

4. Role of external factors

Finally, it would be interesting to judge the relevance of the upper-level PV anomalies relative to the action of other non-internal factors traditionally assumed -and also proved- to be very important in the western Mediterranean flash flood situations, notably the orography and the sea surface latent heat flux. Note that for all the numerical experiments presented in last section, there is a tendency for low pressure developments in the lee of the Atlas mountains, as well as precipitation enhancement in the exposed areas of eastern Spain. This suggests that both local and remote orographies could have played an important role in this case too. On the other hand, the simulations reveal intense evaporation from the warm ($\sim 23^{\circ}\text{C}$) Mediterranean waters during the episode (not shown). For comparison, the control experiment and the basic experiment *S00* were repeated, but eliminating the previous boundary factors (Fig. 8). The first experiment (Fig. 8a) still develops a large cyclone,

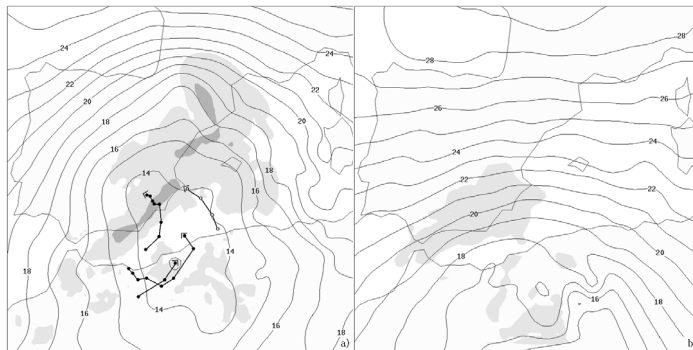


Fig. 8. As in Fig. 2b, except for: (a) Control experiment without both orography and sea surface latent heat flux. (b) Experiment *S00* without both orography and sea surface latent heat flux.

5. Concluding remarks

The western Mediterranean cyclogenesis event of 28-29 September 1994 represents an interesting situation, owing to the presence of two interacting and fast-evolving upper-level positive PV anomalies upstream from the region. The combined application of piecewise PV inversion and numerical simulation offers a valuable and unique framework from which the effects of dynamical features of the flow can be studied in a practical and physically consistent way. In this work, the approach was used to generate an ensemble of mesoscale numerical simulations with perturbed initial intensities or positions of the PV anomalies. The set of hypothetical scenarios so constructed appears to be very useful for investigating the predictability of mesoscale details of the forecast subject to potential errors in the initial representation of the upper-level disturbance.

Acknowledgements

The author acknowledges the support provided by the Scientific Program of NATO for post-doctoral research at the National Severe Storms Laboratory. Precipitation data of the event was provided by the INM of Spain.

but less intense and more circular than in the full simulation (compare with Fig. 2b). Clearly, the effect of the Atlas mountains in modulating the sea level pressure field over the Mediterranean is notable, which implies an enhancement of the impinging easterly moist flow. The general area of precipitation in this modified control experiment does not change strongly, but the amounts are reduced. The output of the modified *S00* experiment (Fig. 8b), to be compared with the results of first panel in Fig. 6, does not even contain any noticeable low pressure centre over the Mediterranean, and the produced precipitation is very weak. In conclusion, the external factors induced an appreciable modulation of the surface circulation and enhanced the efficiency of the system as a rainfall producer, but were not the most essential factors; the cyclogenesis that took place over the southern Mediterranean and its progression to the north must be attributed mostly to the action of the upper-level PV anomalies.

References

- Davis, C. A. and Emanuel, K. A. (1991): "Potential vorticity diagnostics of cyclogenesis". *Mon. Wea. Rev.*, 119, 1929-1953.
- Ertel, H. (1942): "Ein neuer hydrodynamischer wirbelsatz". *Meteor. Z.*, 59, 271-281.
- Grell, G. A., Dudhia, J. and Stauffer, D. R. (1995): *A description of the fifth-generation Penn State/NCAR mesoscale model (MM5)*. NCAR/TN-398+STR, 122 pp.
- Hoskins, B. J., McIntyre, M. E. and Robertson, A. W. (1985): "On the use and significance of isentropic potential vorticity maps". *Quart. J. Roy. Meteor. Soc.*, 111, 877-946.
- Huo, Z., Zhang, D. L. and Gyakum, J. R. (1999): "Interaction of potential vorticity anomalies in extratropical cyclogenesis. Part II: Sensitivity to initial perturbations". *Mon. Wea. Rev.*, 127, 2563-2575.
- Ramis, C., Romero, R., Homar, V., Alonso, S. and Alarcón, M. (1998): "Diagnosis and numerical simulation of a torrential precipitation event in Catalonia (Spain)". *Meteorol. Atmos. Phys.*, 69, 1-21.
- Romero, R., Doswell, C. A. III and Ramis, C. (2000): "Mesoscale numerical study of two cases of long-lived quasistationary convective systems over eastern Spain". *Mon. Wea. Rev.*, 128, 3731-3751.